

A material model of asphalt mixtures based on Monte Carlo simulations

Cite as: AIP Conference Proceedings **2077**, 020057 (2019); <https://doi.org/10.1063/1.5091918>
Published Online: 21 February 2019

Cezary Szydłowski, Jarosław Górski, Marcin Stienss, and Łukasz Smakosz



View Online



Export Citation

ARTICLES YOU MAY BE INTERESTED IN

[Inverse problem in electrochemical machining of rotary surfaces](#)

AIP Conference Proceedings **2077**, 020047 (2019); <https://doi.org/10.1063/1.5091908>

[Extremal thermal loading of a bifurcation pipe](#)

AIP Conference Proceedings **2077**, 020030 (2019); <https://doi.org/10.1063/1.5091891>

[Angular positioning of the object by a system of two backward friction force fields](#)

AIP Conference Proceedings **2077**, 020046 (2019); <https://doi.org/10.1063/1.5091907>

AIP | Conference Proceedings

Get **30% off** all
print proceedings!

Enter Promotion Code **PDF30** at checkout



A material Model of Asphalt Mixtures Based on Monte Carlo Simulations

Cezary Szydłowski^{a)}, Jarosław Górski^{b)}, Marcin Stienss^{c)} and Łukasz Smakosz^{d)}

*Faculty of Civil and Environmental Engineering, Gdansk University of Technology
Narutowicza 11/12, 80-233 Gdansk, Poland*

^{a)}cezszydl@pg.edu.pl

^{b)}Corresponding author: jgorski@pg.edu.pl

^{c)}mstienss@pg.edu.pl

^{d)}luksmako@pg.edu.pl

Abstract. The paper aims to numerically reflect mineral-asphalt mixture structure by a standard FEM software. Laboratory test results are presented due to bending tests of circular notched elements. The result scatter is relatively high. An attempt was made to form a random aggregate distribution in order to obtain various results corresponding to laboratory tests. The material structure calibration, its homogenization and finite element dimensioning are the issues decisive for the objective mixture description. The representative volume element (RVE) is investigated here, while it does not precisely reflect the material structure it displays relevant global material parameters. The simulation procedure applied here makes it possible to introduce the name of Monte Carlo simulation-based constitutive model.

INTRODUCTION

Fracture phenomenon of asphalt mixtures acts strongly on the costs of road construction and repair and on traffic safety. While fracture mechanisms have not been relevantly recognized yet, attempts have been provided to incorporate them in the design process [1, 2, 3]. It seems a considerable task due to highly complex constitutive relations regarding temperature, aggregate layout, crack onset and propagation and more factors.

The laboratory tests regarding asphalt mixture research should be supported by computational work. The FEM analytical variants correspond to various levels of material reflection: mesoscale, multiscale, continuum approaches and others [4 - 11]. The models of improved precision require additional experimental data to reflect e.g. the contact between aggregate and bituminous material. It seems more effective to find out simple, less time-consuming homogenization models of complex material contents of asphalt mixtures. Such a solution, tested on laboratory pieces, seems effective in the modelling of larger parts of road pavements.

The simplified approach to non-homogeneous materials takes a supporting analysis involving the definition of a representative volume element (RVE) [4, 12 - 15]. A dedicated computer simulation is aimed at reflecting a random character of asphalt mixture [4, 10, 13, 14, 16 - 20]. It concerns both aspects of material parameter dispersion and aggregate layout in the test piece volume. Random material modelling is the main issue of the work, to be later called Monte Carlo constitutive equations.

The work incorporates a quasi-continuum model to reflect fracture of notches elements. The ABAQUS software was applied here, incorporating its built-in standard procedures. However the simulation of random aggregate layout is performed by means of separate, author's software. The material parameters are assessed on the basis of the author's experimental research. The test domain was limited to the temperatures below zero, denoting a brittle fracture pattern.

There are available few fracture models in ABAQUS software, e.g. smeared crack model or cohesive link model. Cohesive elements may be easily introduced in the regions of detected crack course. This is the approach incorporated in the work.

LABORATORY TESTS

The laboratory tests to estimate fracture parameters of a mineral-asphaltic mix were conducted in the laboratory of the Department of Highway Engineering at the Faculty of Civil and Environmental Engineering, Gdańsk University of Technology [16]. Semi-circular test pieces subjected to three-point bending were applied (Figure 1) according to the PN-EN 12697-44 standard. Vertical deflections d and forces F were measured experimentally. The displacement rate was 1 mm/min. In the test course specimen and loading frame were located in thermostatic chamber of the press to achieve a constant target test temperature equal -20°C . The tests were performed considering three notch depth cases, i.e. $a = 10$ mm, 20 mm, 30 mm. Two types of asphalt mixtures due to wearing course were regarded, i.e. stone matrix asphalt SMA 8 and porous asphalt PA 8. The work presents the results of the PA 8 mixture only (Figure 2, Table 1).

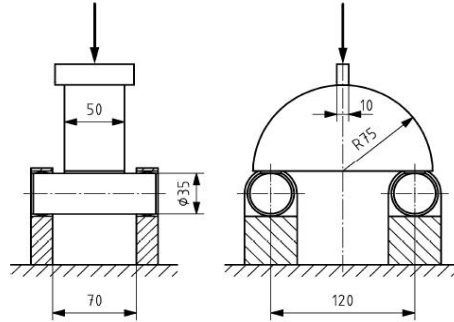


FIGURE 1. Semi-circular specimens.



FIGURE 2. Stone matrix asphalt PA 8.

Table 1. Composition of tested asphalt mixtures.

| | Passes # [mm] | PA8 Mixture |
|-----------|---------------------|-------------|
| Aggregate | 11.2 | 100 |
| | 8 | 91.2 |
| | 5.6 | 13.4 |
| | 2 | 6.7 |
| | 0.125 | 4.8 |
| | 0.063 | 4.1 |
| Bitumen | optimum content [%] | 6.5 |
| | type of bitumen | 45/80-65 |

The laboratory test results are summarized in Table 2. Four samples were tested in each case. Figure 3 presents load F vs. deflection d curves in the case of four tested samples featuring $a = 20$ mm notches. The results show high dispersion in maximum forces F and in the linear part slope ($\tan \alpha$) on the force–deflection ($F - d$) diagram (Figure 3). This observation is reflected in standard deviations (SD) and coefficients of variation (CV) of relevant variables (Table 2). Considering the case of mixture PA 8 and a 20 mm notch - in the maximum force region the coefficient of variation is estimated 0.08 while in the linear diagram part the coefficient of variation is estimated 0.13. These values are relatively high, so laboratory test documentation should be supplemented by statistical analysis, in numerical computation probabilistic approach should be introduced as well.

Table 2. The results of fracture toughness test at -20°C - PA 8 mixture.

| a [mm] | F_{max} [N] | | | | $Tan\alpha$ [N/mm] | | | |
|-------------|---------------|------|-----|--------|--------------------|-------|------|--------|
| | sample | mean | SD | CV [%] | sample | mean | SD | CV [%] |
| 10 | 4894 | 5220 | 462 | 9 | 17594 | 23396 | 5933 | 25 |
| | 5550 | | | | | | | |
| | 5678 | | | | | | | |
| | 4756 | | | | | | | |
| 20 | 3280 | 2968 | 241 | 8 | 11552 | 11857 | 1593 | 13 |
| | 2700 | | | | | | | |
| | 2902 | | | | | | | |
| | 2988 | | | | | | | |
| 30 | 807 | 1517 | 475 | 31 | 10131 | 8154 | 2658 | 33 |
| | 1741 | | | | | | | |
| | 1816 | | | | | | | |
| | 1703 | | | | | | | |

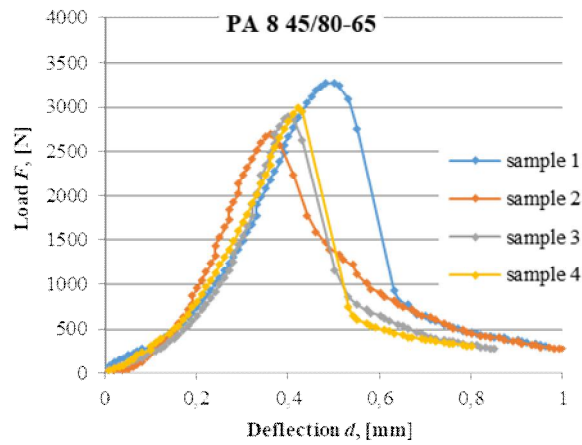


FIGURE 3. Laboratory test results for notch depth 20 mm.

MONTE CARLO MATERIAL MODEL

In order to reflect random mechanical response of the material a numerical model was proposed incorporating Monte Carlo sampling. Assumption was made to link specific FEM elements with material parameters of aggregate or bitumen mortar, according to the contribution percentage. It is also possible to fill in the sample volume with voids (Fig. 4). The dedicated software code was created to form the FEM model corresponding to the input data ABAQUS code. While material features of single elements are generated it is possible to reflect diverse sample stiffness caused by diversity of aggregate distribution.

An additional factor leading to the choice of aggregate distribution is the possibility to join elements in larger groups, of a number of four or more (Fig. 4). Such assemblies are possible in the case of a significantly dense FE mesh.

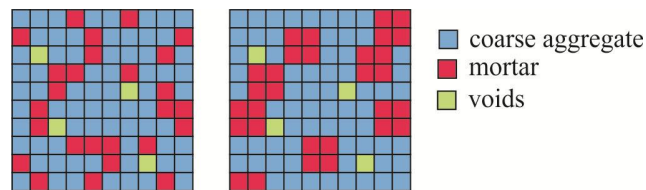


FIGURE 4. Random aggregate distributions: one element and four elements.

Parameter calibration is conducted by an axially compressed specimen (Fig. 5). Both specimen dimensioning and FE mesh adjustment are decisive to the computational results. The algorithm is not aimed at reflecting a real material, instead, it replaces the real material by a quasi-homogenized structure, showing its mechanical response convergent with the laboratory results. Such a simplified approach makes it possible to find the scatter of global element bending stiffness EI .

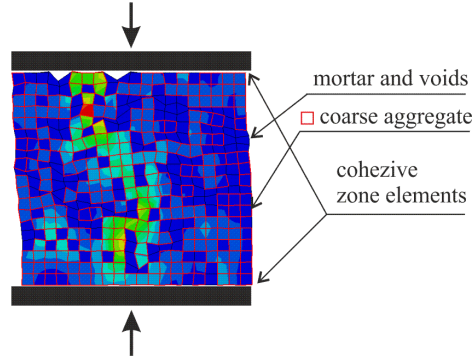


FIGURE 5. Axially compressed specimen.

Global Young's modulus variation was investigated, given various ingredient proportions. The following material data were initially assumed: Young's modulus of aggregate $E_{ag} = 80000$ MPa and bituminous mortar $E_m = 80$ MPa, percentage of aggregate content from 100% to 50%. Figure 6 presents the results corresponding to variable percentage of aggregate content.

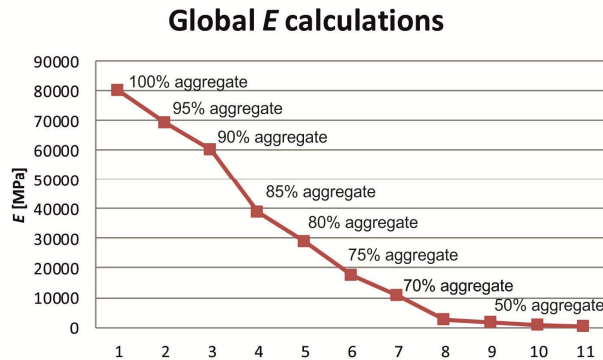


FIGURE 6. Global E calculation with regard to various percentage of aggregate content.

Next, with regard to selected data $E_{ag} = 80000$ MPa, 60% of aggregate content and $E_m = 80$ MPa the tests were undertaken of the element global Young's modulus variation due to various generated aggregate distributions. An entirety of 10 tests led to the following Young's modulus parameters: mean value 1802 MPa and standard deviation 225 MPa. Figure 7 presents stress distributions corresponding to three random samples. The observable stress transformation process is caused by randomly distributed aggregate.

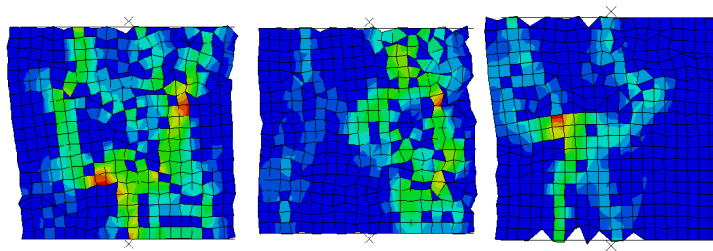


FIGURE 7. Samples of generated aggregate dispersions - stress fields under uniform compression.

The generation can be sequentially repeated, to finally get the material by means of Young's modulus mean value and standard deviation, both based on experiments. Thus the process may be called Monte Carlo simulation-based constitutive relations.

FEM CALCULATIONS

The presented numerical analysis is preliminary. Generation of random scatter of material parameters was not performed here. The computations were conducted in the ABAQUS environment [22]. Cohesive models were chosen from a variety of standard models to feature the axial specimen part (Fig. 8a). The essential analytical part is a relevant selection of material parameters (Fig. 8b) and other parameters referring to cohesive elements. While an entire data set to cover both aggregate and bitumen is not accessible a series of tests was conducted to adjust the FEM results to experimental relations. Hence the implemented model is phenomenological in its character.

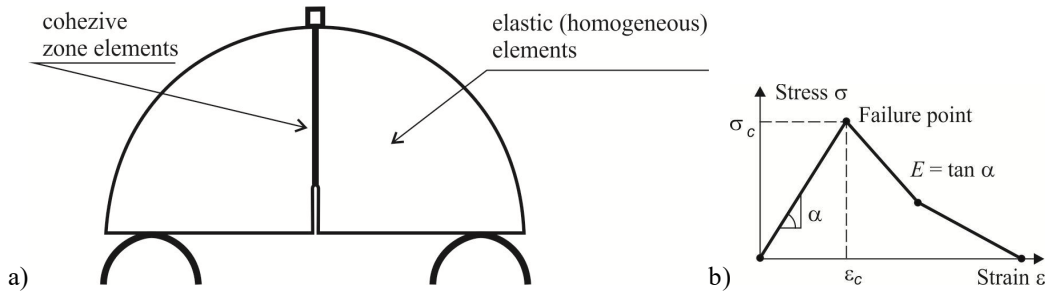


FIGURE 8. Cohesive element crack model (a) and $\sigma - \varepsilon$ constitutive relation in tension (b).

The model calibration was provided due to the PA8 mix specimen with a 20 mm notch. The laboratory test results (Fig. 3) led to the simplest elastic-brittle material model. In this example the asphalt mix was assumed homogeneous. The results in Table 2 brought about the following averaged continuum parameters: $E = 1$ GPa, $\nu = 0.2$. The cohesive element parameters are: traction separation behaviour $K_{nn} = K_{ss} = K_{tt} = 10^{-12}$, total plastic displacement = 0.0001, damage stabilization (viscosity coefficient) = 0.0001. The cohesive FEM model and the propagation of crack are presented in Fig. 9. The obtained satisfactory results due to the 20 mm notch case are shown in Fig. 10.

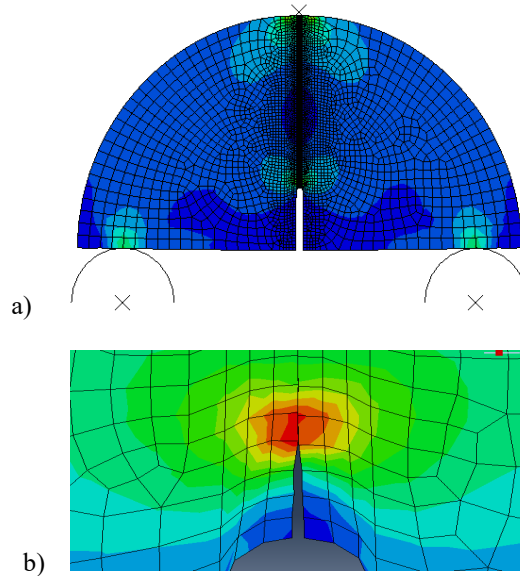


FIGURE 9. Cohesive element crack model: sample mesh (a), and propagation of crack (b).

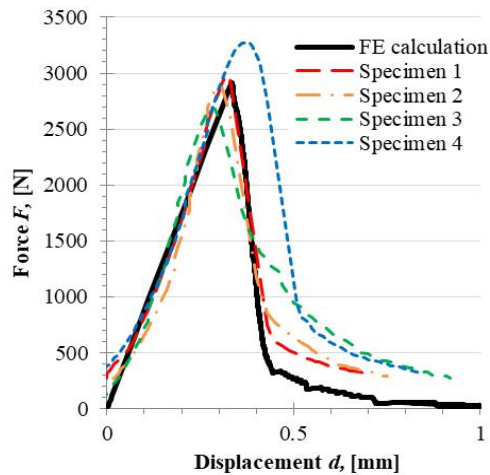


FIGURE 10. Comparison of experimental results and FE calculations – diagram $F-d$, 20 mm notches.

The same material input data were applied to analyse the test pieces with notches equal 10 mm and 30 mm. The results are presented in Fig. 11. The experimental research was reflected sufficiently well. These results did not cover the material data scatter, i.e. the material was assumed homogeneous.

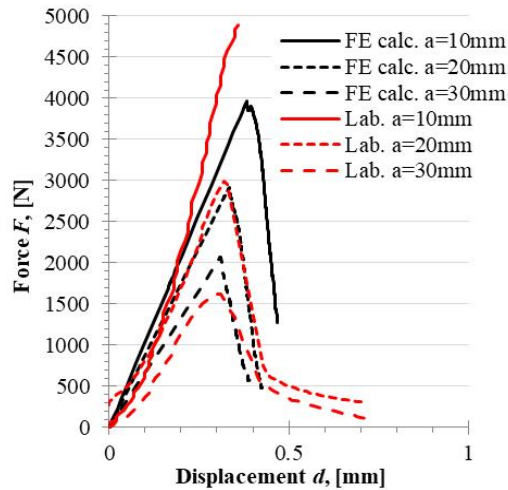


FIGURE 11. Comparison of experimental results and FE calculations – diagram $F-d$ for the PA 8 asphalt mixture.

CONCLUSIONS

The entirety of laboratory experiments and numerical analysis shows its preliminary character.

The complete result set should consider crack mouth opening displacement (CMOD) to find out diagrams in the weakening (softening) region too.

The generation of random scatter of material parameters requires relevant calibration regarding e.g. finite element dimensions. However, the presented preliminary computations show the way to directly apply the Monte Carlo method in material parameter modelling.

REFERENCES

1. T. L. Anderson, *Fracture mechanics fundamentals and applications*(Taylor & Francis, 2005).
2. Y. R. Kim, *Modelling of asphalt concrete*(ASCE Press Mc GrawHil, 2009).

3. L. Wang, *Mechanics of asphalt Microstructure and micromechanics*(ASCE Press Mc GrawHil, 2011).
4. J. Wimmer, B. Stier, J.W. Simon and S. Reese, *Finite Elements in Analysis and Design* **110**, pp. 43–57 (2016).
5. H. Wang, J. Wang, J. Chen, *Engineering Fracture Mechanics* **132**, pp. 104–119 (2014).
6. T. You, R. K. A. Al-Rub, M. K. Darabi, E. A. Masad and D. N. Little, *Construction and Building Materials* **28**, pp. 531–548 (2012).
7. K. H. Moon, A. C. Falchetto and J. W. Hu, *Construction and Building Materials* **53**, pp. 568–583 (2014).
8. E. Mahmoud, S. Saadeh, H. Hakimelahi and J. Harvey, *Road Materials and Pavement Design* **15**(1), pp. 153-166 (2013).
9. A. Yin, X. Yang, S. Yang and W. Jiang, *Engineering Fracture Mechanics* **78**, pp. 2414-2428 (2011).
10. T. Schüler, R. Jänicke and H. Steeb, *Construction and Building Materials*, pp. 96-108 (2016).
11. X. Li and M. O. Marasteanu, *International Journal of Fracture* **136** pp. 285–308 (2005).
12. M. Galouei, A. Fakhimi, *Computers and Geotechnics* **65** pp. 126–135 (2015).
13. .T. Kanit, S. Forest, I. Galliet, V. Mounoury, D. Jeulin, *International Journal of Solids and Structure* **40** pp. 3647–3679 (2003).
14. M. Ostoja-Starzewski, *Probabilistic Engineering Mechanics* **21** pp. 112-132 (2006).
15. T. Pellinen, E. Huuskonen-Snicker, P. Eskelinen, P. O. Martinez, *Journal of traffic and transportation engineering* **2**(1), pp. 30-39 (2015).
16. C. Szydłowski, J. Judycki, *Highway Engineering* **10**, pp. 348–353 (2015) (in Polish).
17. S.-J. Lee, G. Zi, S. Mun, J. S. Kong, J.-H. Choi, *Engineering Fracture Mechanics* **141** pp. 212–229 (2015).
18. A. Yin, X. Yang, H. Gao, H. Zhu, *Engineering Fracture Mechanics* **92** pp. 40–55 (2012).
19. X. F. Wang, Z. J. Yang, J. R. Yates, A. P. Jivkov, C. Zhang, *Construction and Building Materials* **75** pp. 35–45 (2015).
20. X. Wang, Z. Yang, A. P. Jivkov, *Construction and Building Materials* **80** pp. 262–272 (2015).